Proceedings of the 11th World Congress on Mechanical, Chemical, and Material Engineering (MCM'25)

Paris, France - August, 2025 Paper No. HTFF 159 DOI: 10.11159/htff25.159

Preliminary CFD Study of a Gyroid-Based Recuperator for Sco₂ Power Cycles

Alexandre Guille¹, Sebastian Unger¹, Uwe Hampel^{1,2}

¹Helmholtz-Zentrum Dresden-Rossendorf, Bautzner Landstraße 400, Dresden, Germany a.guille-bourdas@hzdr.de; s.unger@hzdr.de

²Technische Universität Dresden, 01069, Dresden, Germany u.hampel@hzdr.de

Abstract – Supercritical CO_2 power cycles have been recently studied for their high efficiency, but each component deserves careful investigation. Among these, the recuperator significantly increases the cycle efficiency by recovering the heat from the turbine outlet. At the Helmholtz-Zentrum Dresden-Rossendorf, the use of Triply Periodic Minimal Surfaces (TPMSs) as internal structures was investigated. Although TPMSs have been broadly studied in material science, their performance in heat transfer between two supercritical fluids remains underexplored. Numerical simulations are essential to assess the heat transfer and pressure drop mechanisms in such complex geometries. This study presents a preliminary Computational Fluid Dynamics (CFD) investigation of sCO_2 flow around a gyroid heat exchanger structure within a counterflow configuration. The analysis mainly focuses on heat transfer between hot sCO_2 at 75 bar and 447 °C on one side and cold sCO_2 at 250 bar and 113 °C on the other side, considering different velocities, wall thicknesses, and periodic lengths. It was found, that the heat transfer coefficient on both sides is equal, in agreement with the Reynolds analogy. An example of correlation, based on power laws, is proposed with an accuracy of \pm 20%. However, significant deviations are observed at low velocities, suggesting either a change of flow regime, a limited application of the used turbulent model or inadequate definition of the heat transfer coefficient. Future investigations will include comparison with experimental data and a local approach of the heat transfer coefficient and pressure drop.

Keywords: Supercritical CO₂; sCO₂ power cycle; Recuperator; Heat transfer; Triply periodic minimal surface; CFD simulation.

1. Introduction

Supercritical CO₂ (sCO₂) power cycles have drawn significant attention in electricity generation due to their higher efficiency compared to conventional cycles [1]. When CO₂ reaches supercritical conditions at 31.0 °C and 73.8 bar, its viscosity decreases while maintaining high density, increasing thermal performance. Dostal et al. [2] showed that sCO₂ power cycle efficiency is higher than a traditional water-based Rankine power cycle when the inlet temperature exceeds 550 °C. Various cycle layouts have been assessed to further enhance efficiency by considering more components [3]. Fig. 1 illustrates the simplest configuration, denoted as the simple recuperated cycle.

The recuperator is a major component in sCO_2 power cycles, recovering energy from the low-pressure, between 75 and 100 bar, hot fluid and transferring it to the high-pressure, between 200 and 300 bar, cold fluid before it enters the turbine. As CO_2 remains supercritical on both sides, channels with a characteristic hydraulic diameter of around 1 mm are used to exploit its low viscosity. Various channel geometries have been studied in the literature to enhance heat transfer while minimizing pressure drops [4].

Triply Periodic Minimal Surfaces (TPMSs) are known structures for their excellent mechanical properties [5], but their usage in heat transfer has received only recent attention [6]. Before experimenting with TPMS structures with sCO₂, further numerical simulations using Computational Fluid Dynamics (CFD), such as the work of Li et al. [7], are necessary to understand the heat transfer mechanism in such complex heat exchanger structures.

In this paper, a particular type of TPMS, the gyroid surface, is investigated as a potential structure for the recuperator in an sCO₂ power cycle. The methodology for generating CFD domains is presented, followed by preliminary simulation results and analysis. Finally, an attempt for proposing a heat transfer correlation is made and its validity is discussed.

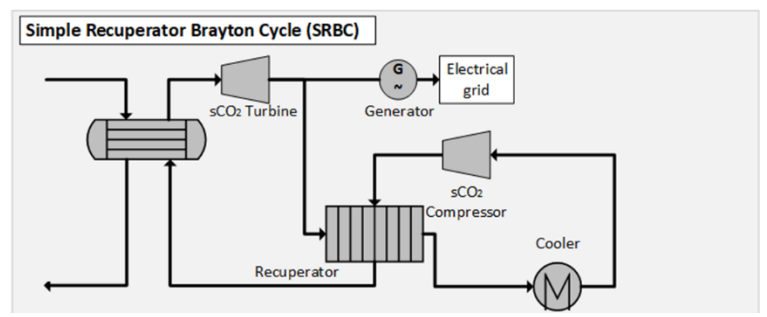


Fig. 1: Layout of simple recuperated sCO₂ power cycle.

2. CFD simulation

2.1. Geometry generation

The gyroids can be mathematically approximated by an implicit function as

$$F(x,y,z) = \sin\left(\frac{2\pi}{L}x\right)\cos\left(\frac{2\pi}{L}y\right) + \sin\left(\frac{2\pi}{L}y\right)\cos\left(\frac{2\pi}{L}z\right) + \sin\left(\frac{2\pi}{L}z\right)\cos\left(\frac{2\pi}{L}x\right)$$
(1)

where L is the periodic length in all the directions. This equation is injected into the free software MSLaticce [8] under the following form:

 $F(x,y,z) = t^*$ (2) where t^* is the dimensionless thickness, which is a value used to thicken the wall of the solid body. After generating one cell in .stl format, the cell is loaded in SpaceClaim, where it is cleaned, scaled to the proper dimension and turned into CAD format (Fig. 2). The number of cells in this study is constant, set at 6 cells. Then, the fluid domains for the hot and cold channels are generated by filling the empty space with material. More bodies are added at the inlets and outlets of both fluids to ensure that the velocity and temperature fields are not influenced by the boundary effects.

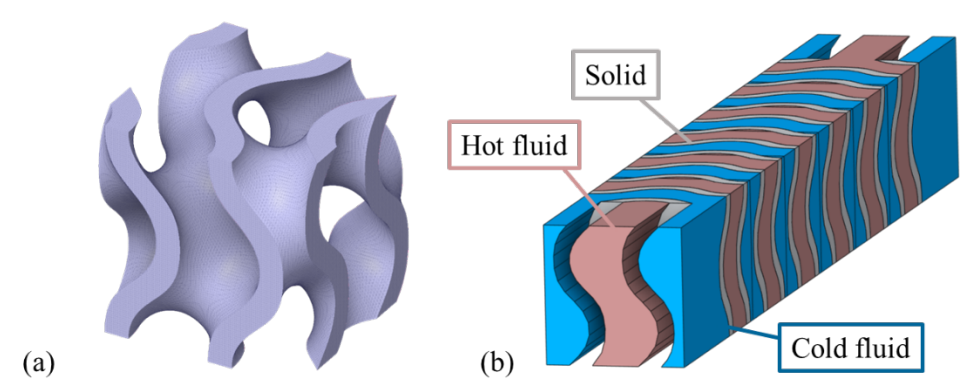


Fig. 2: (a) Cell generated in MSLaticce and (b) turned into CAD format along with the fluid domains.

Once the solid and fluid domains are generated in CAD format, they are imported in *Fluent Meshing* to be meshed. Given the geometry complexity, polyhedra elements are adopted. Inflation layers are attached to the walls to capture the boundary layer, as seen in Fig. 3.

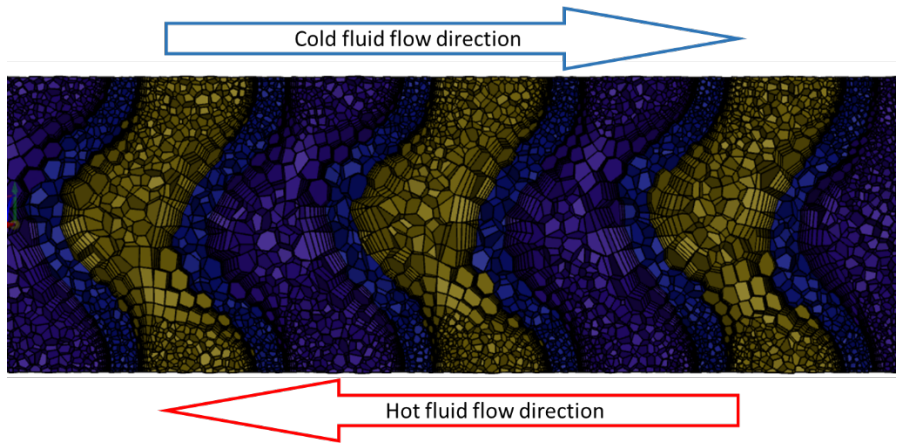


Fig. 2: Sectional view of the mesh close to the wall.

2.2. Flow equations

The study focuses on the heat transfer of both fluids in steady state conditions, therefore, a Reynolds-averaged approach is adopted in this investigation. The equations on the field components are formulated as

$$\frac{\partial}{\partial x_i} (\rho u_i) = 0 \tag{3}$$

$$\frac{\partial}{\partial x_{i}} (\rho u_{i}) = 0$$

$$\frac{\partial}{\partial x_{j}} (u_{i}u_{j}) = -\frac{\partial p}{\partial x_{i}} + \frac{\partial}{\partial x_{j}} \left[(\mu + \mu_{t}) \left(\frac{\partial u_{i}}{\partial x_{j}} + \frac{\partial u_{j}}{\partial x_{i}} \right) \right]$$

$$(4)$$

$$\frac{\partial}{\partial x_{j}} \left(\rho u_{j} H \right) = \frac{\partial}{\partial x_{j}} \left[\lambda \frac{\partial T}{\partial x_{j}} + \frac{\mu_{t} \partial h}{P r_{t} \partial x_{j}} \right] \tag{5}$$

where ρ is the fluid density, λ is the fluid conductivity, μ is the fluid viscosity, H is the fluid enthalpy, and μ_t is the turbulent viscosity. They are functions of temperature and pressure and calculated in this study with the Python wrapper CoolProp [9]. The SST $k-\omega$ turbulence model is used to calculate μ_t and close the equations, and Pr_t is set at 0.85. This leads to having a very fine mesh near the wall to achieve the condition $y^+ \approx 1$. The case is set up in *Fluent*, where the coupled scheme is used for its robustness, along with second-order upwind for the spatial discretization of all other variables. Periodic boundary conditions are applied on each side of the solid and fluid domains. The solid body is assumed to be made of aluminum, and thus the corresponding material properties were applied.

The variables of interest, including temperature and pressure, are averaged across planes at the inlet and outlet of the fluid domains. The heat transfer coefficient, however, is calculated by averaging the surface heat transfer coefficients on the hot and cold walls. The reference temperature is determined by the nearest cell in *Fluent*, and this choice is discussed later.

3. Results and discussion

This part presents the preliminary results of the simulation of a recuperator with sCO₂ as both hot and cold fluids. The hot fluid is at the lowest pressure, 78 bar, because it exits the turbine (Fig. 1). On the other hand, the cold fluid exits the compressor at 250 bar, thus showing the highest operating pressure. Table 1 summarizes the thermal boundary conditions that are constant in the simulation. One missing data is the inlet velocities. Since they depend on the total heat duty and the total size of the recuperator, they are studied here over a certain range. Nonetheless, mass flow rates in both channels are equal. Indeed, in the simple recuperated power cycle, the flow is not split before entering the recuperator, hence the mass flow rates are equal. In addition, the cross-sectional surface areas are equal due to the shape of the gyroids, leading the mass flow rate assumption to be expressed as:

$$\rho_{hot} u_{hot} = \rho_{cold} u_{cold} \tag{6}$$

where ρ_{hot} is lower due to the lower pressure, thus the velocity in the hot channel u_{hot} is higher, with a ratio $u_{cold}/u_{hot} \approx 0.108$. Table 2 presents the range of the parameters that vary in this study.

Table 1: Thermal boundary conditions necessary to run the simulations.

Boundary conditions	T _{hot,in}	T _{cold,in}	P _{hot,out}	P _{cold,in}
Value	447 °C	113 °C	78 bar	250 bar

Table 2: Range of parameter study.

Parameter range	u _{hot,in}	u _{cold,in}	L	t^*
Value	1 - 10 m/s	0.108 - 1.08 m/s	1 – 12 mm	0.2 - 0.6

Fig. 4 shows the velocity and temperature fields on the XZ plane at y = 0 mm, where x is the flow direction. The length L is set to 4 mm, t^* is set to 0.4, and the velocity is set at 5 m/s at the hot fluid inlet. Figure 4a shows that the maximum velocity occurs in the hot channels, where the inlet velocity is higher for a comparable mass flow rate. The peak value reaches 17.4 m/s, which is 3.48 times the inlet velocity. However, these are local peaks, which may be strongly influenced by the mesh resolution. Besides that, the majority of the velocity values are around 8 m/s, which is only 1.6 times the inlet velocity. Due to the relation presented in Eq. 6, the maximum velocity in the cold channel does not reach more than 1.7 m/s. In Fig. 4b, a more visible temperature gradient is observed from the inlet to the outlet of both fluids. The temperature in the cold channel increases as the temperature in the hot channel decreases, which is due to the counterflow configuration. In the solid region, the temperature is more uniformly distributed, ranging from 213 °C to 260 °C.

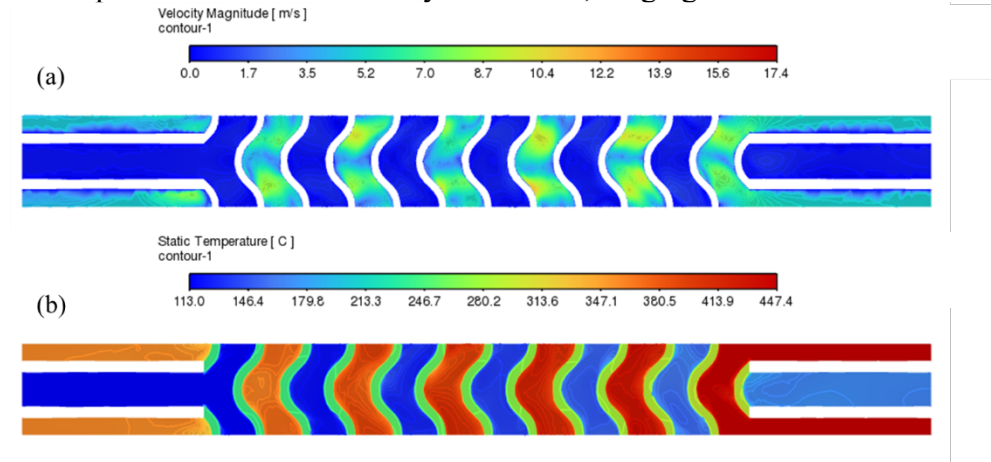
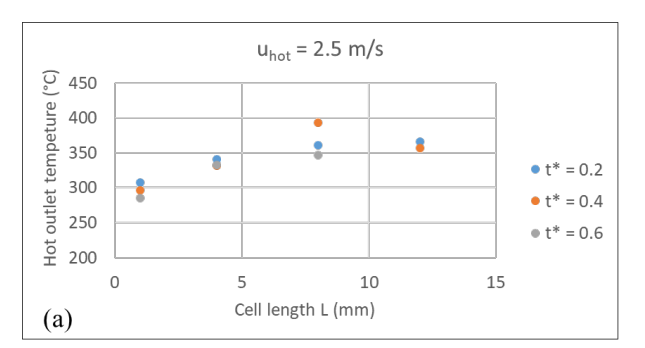


Fig. 4: (a) Velocity field and (b) temperature field along the flow direction.

Fig. 5a plots the outlet temperature of the hot fluid for different periodic lengths at fixed inlet velocities. u_{hot} is set at 2.5 m/s, thus u_{cold} is equal to 0.27 m/s (Eq. 6). The hot outlet temperature increases with L, and stagnates from 8 mm. As L increases, the heat exchange surface area grows due to a constant number of cells. However, Fig. 5b shows that the heat transfer coefficient in the hot channel decreases with L until it stagnates at 8 mm, indicating that there are fewer disturbances in the flow.

It both figures, different thicknesses are considered. It can be seen that, apart from the geometry corresponding to L equal to 8 mm and t^* equal to 0.4, the values are almost identical. It suggests that thickness has negligible effect on the heat transfer in gyroids.



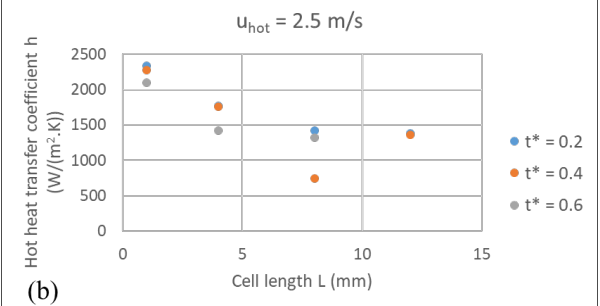


Figure 5: (a) Evolution of heat transfer coefficients for one geometry as a function of fluid velocity in the hot channel as reference. (b) Comparison between heat transfer coefficients calculated by CFD and through the correlation of Eq. (9).

Fig. 6a plots the evolution of the heat transfer coefficient for both fluids, which increases with velocity due to higher turbulence. Despite differences in velocity and pressure, the coefficients remain similar. This may be attributed to equal mass flow rates (Eq. 6) and identical hydraulic diameter. For instance, at 280 °C, the viscosities of sCO₂ at 78 bar and 250 bar are 2.72×10⁻⁵ Pa.s and 3.19×10⁻⁵ Pa.s, respectively, leading to a higher Reynolds and Nusselt number in the hot channel. However, the higher thermal conductivity of the cold fluid, 0.048 compared to 0.040 W/(m·K), compensates for this effect, resulting in comparable heat transfer coefficients. Following this idea, an attempt to formulate the heat transfer coefficient as a function of the different parameters involved in this study is given in Eq. 9. The power-law approach was used to develop the correlation, the coefficient attributed to the thickness effect, evaluated at -0.02, is very low compared to the others in agreement with the results found with Fig. 5. A plot showing the difference between the heat transfer coefficients calculated by CFD and by the correlation. It can be seen that most of the points stayed within the range of \pm 20%. However, for low coefficients, below 1000 W/(m².K), CFD results deviate significantly. It may be due to a different regime, but it was found that a heat imbalance occurred only at low velocities, especially in the cold fluid. Further investigations are required, including experimental work planned at HZDR in 2025, better mesh validation, and the use of turbulence models adaptable to laminar regimes. Additionally, a more accurate formulation of the heat transfer coefficient is needed, as the reference temperature is currently based on the nearest mesh rather than the bulk temperature.

$$Re = \frac{\rho u d_h}{\mu}$$

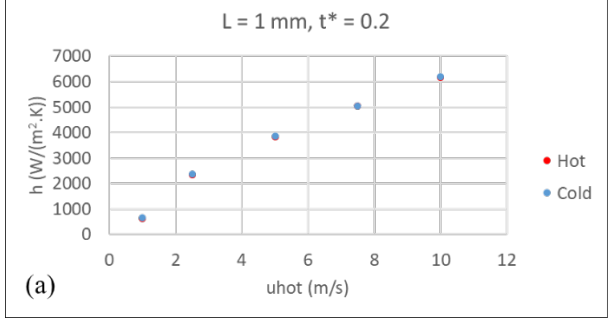
$$Nu(Re) = \frac{h d_h}{\lambda}$$

$$h = 1018 * L^{-0.274} * u_{hot}^{0.779} * t^{*-0.02}$$
(8)

$$Nu(Re) = \frac{hd_h}{a} \tag{8}$$

$$h = 1018 * L^{-0.274} * u_{hot}^{0.779} * t^{*-0.02}$$

$$\tag{9}$$



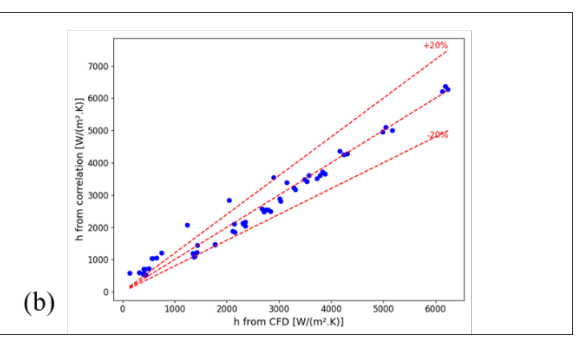


Figure 6: (a) Evolution of heat transfer coefficient for one geometry as a function of fluid velocity in the hot channel as reference. (b) Comparison between heat transfer coefficients calculated by CFD and through the correlation of Eq. (9).

4. Conclusion

In the present study, the flow of sCO₂ in a recuperator filled with a certain type of TPMSs, the gyroid surface, was numerically studied by CFD. Simulations were carried out for varying periodic lengths, wall thicknesses, and inlet velocities. Although preliminary, the results allowed for an initial evaluation of heat transfer between the two fluids. The periodic length has a large impact on the heat performance but the thickness has negligible impact. The heat transfer coefficient was found to be similar for both hot and cold streams at equal mass flow rates, consistent with the Reynolds analogy. As a result, a power law correlation applicable to both fluids was proposed. However, the correlation appears to deviate at low velocities, where the flow may change the regime and the definition of the heat transfer coefficient may be less reliable.

Acknowledgements

This research is part of the project ESCO funded by the German Federal Ministry for Economic Affairs and Climate Action (BMWK) under the grant number 03EE5157H. Responsibility if the content of this publication lies with the authors.

References

- [1] J. Xu, C. Liu, E. Sun, J. Xie, M. Li, Y. Yang, and J. Liu, "Perspective of S-CO2 power cycles," *Energy*, vol. 186, p. 115831, Nov. 2019, doi: 10.1016/J.ENERGY.2019.07.161.
- [2] V. Dostal, P. Hejzlar, and M. J. Driscoll, "The supercritical carbon dioxide power cycle: Comparison to other advanced power cycles," *Nucl Technol*, vol. 154, no. 3, 2006, doi: 10.13182/NT06-A3734.
- [3] Y. Liu, Y. Wang, and D. Huang, "Supercritical CO2 Brayton cycle: A state-of-the-art review," 2019. doi: 10.1016/j.energy.2019.115900.
- [4] C. Huang, W. Cai, Y. Wang, Y. Liu, Q. Li, and B. Li, "Review on the characteristics of flow and heat transfer in printed circuit heat exchangers," 2019. doi: 10.1016/j.applthermaleng.2019.02.131.
- [5] N. Qiu, Y. Wan, Y. Shen, and J. Fang, "Experimental and numerical studies on mechanical properties of TPMS structures," *Int J Mech Sci*, vol. 261, p. 108657, Jan. 2024, doi: 10.1016/J.IJMECSCI.2023.108657.
- [6] W. Li, G. Yu, and Z. Yu, "Bioinspired heat exchangers based on triply periodic minimal surfaces for supercritical CO2 cycles," *Appl Therm Eng*, vol. 179, p. 115686, Oct. 2020, doi: 10.1016/J.APPLTHERMALENG.2020.115686.
- [7] W. Li, W. Li, and Z. Yu, "Heat transfer enhancement of water-cooled triply periodic minimal surface heat exchangers," *Appl Therm Eng*, vol. 217, p. 119198, Nov. 2022, doi: 10.1016/J.APPLTHERMALENG.2022.119198.
- [8] O. Al-Ketan and R. K. Abu Al-Rub, "MSLattice: A free software for generating uniform and graded lattices based on triply periodic minimal surfaces," *Material Design and Processing Communications*, vol. 3, no. 6, 2021, doi: 10.1002/mdp2.205.
- [9] I. H. Bell, J. Wronski, S. Quoilin, and V. Lemort, "Pure and pseudo-pure fluid thermophysical property evaluation and the open-source thermophysical property library coolprop," *Ind Eng Chem Res*, vol. 53, no. 6, 2014, doi: 10.1021/ie4033999.